

# Reducing self-supervised learning complexity improves weakly-supervised classification performance in computational pathology

Tim Lenz<sup>1</sup>, Omar S. M. El Nahhas<sup>1</sup>, Marta Ligeró<sup>1</sup>, and  
Jakob Nikolas Kather<sup>1,2,3</sup>

<sup>1</sup> Else Kroener Fresenius Center for Digital Health, Medical Faculty Carl Gustav Carus, TUD Dresden University of Technology, Germany

<sup>2</sup> Department of Medicine 1, University Hospital and Faculty of Medicine Carl Gustav Carus, TUD Dresden University of Technology, Germany

<sup>3</sup> Medical Oncology, National Center for Tumor Diseases (NCT), University Hospital Heidelberg, Heidelberg, Germany

**Abstract.** Deep Learning models have been successfully utilized to extract clinically actionable insights from routinely available histology data. Generally, these models require annotations performed by clinicians, which are scarce and costly to generate. The emergence of self-supervised learning (SSL) methods remove this barrier, allowing for large-scale analyses on non-annotated data. However, recent SSL approaches apply increasingly expansive model architectures and larger datasets, causing the rapid escalation of data volumes, hardware prerequisites, and overall expenses, limiting access to these resources to few institutions. Therefore, we investigated the complexity of contrastive SSL in computational pathology in relation to classification performance with the utilization of consumer-grade hardware. Specifically, we analyzed the effects of adaptations in data volume, architecture, and algorithms on downstream classification tasks, emphasizing their impact on computational resources. We trained breast cancer foundation models on a large public patient cohort and validated them on various downstream classification tasks in a weakly supervised manner on two external public patient cohorts. Our experiments demonstrate that we can improve downstream classification performance whilst reducing SSL training duration by 90%. In summary, we propose a set of adaptations which enable the utilization of SSL in computational pathology in non-resource abundant environments.

**Keywords:** Self-Supervised Learning · Pathology · Foundation Models.

## 1 Introduction

Artificial Intelligence (AI) tools can assist pathologists in various tasks like tumor detection [26], disease classification [27] or prognosis [16] and has even enabled the extraction of clinically actionable insights from routinely available data [23].

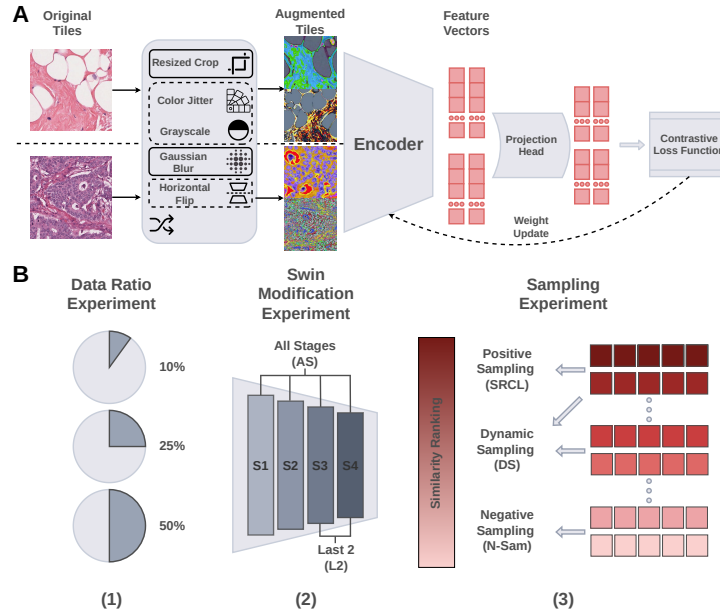


**Fig. 1. Experiment Overview.** (A) visualizes the contrastive SSL algorithm. (B) shows an overview of the experiments we performed in this study. (1) We train on subsets of the SSL data to analyze the impact of reduced data volumes during SSL on downstream classification performance (DCP). (2) We investigate the DCP of feature vectors retrieved from earlier stages of our SSL trained tiny Swin Transformer as well as combined feature representations of multiple layers. (3) We propose semantically relevant sampling methods to improve contrastive SSL in histopathology. Hence, for each feature representation of an input sample we rank all other representations of a batch based on the cosine similarity. Subsequently, we retrieve certain subsets of this ranking and adapt their weight in the contrastive loss function.

Traditionally, the development of AI models for medical applications has relied heavily on manually annotated data [21]. Foundation models for computational pathology have proven to alleviate the need for annotated data as they are pre-trained on diverse datasets in order to be applied on various different use cases that are relevant for current research [28]. In order to obtain adequate foundation models, massive amounts of data and compute are utilized [3, 4, 9, 24] to train large scale models like Vision Transformers (ViTs) [8]. The amount of training data can be substantially increased if the necessity of annotations is avoided. This led to the establishment of SSL methods [3]. Instead of focusing on few targets during training, SSL methods learn from inherent patterns and relationships in unlabeled data. Thereby, the capacity for generalization and adaptation to diverse tasks is amplified, while also surpassing the performance of models trained in a supervised manner [5, 7, 11, 12]. Foundation models trained with SSL methods are often applied as encoders to compress the high-dimensional

input data to its most important information content in the form of feature vectors. Those feature vectors are then applied on downstream classification tasks in a weakly supervised manner [23]. The rise of SSL methods alongside exponential hardware improvements enabled the training of increasingly capable foundation models. Nevertheless, current strategies are too resource-intensive as the data volumes, hardware requirements and overall costs are increasing rapidly to a point where only few institutions can contribute to methodological improvements in this field of research. This point is exemplified in recent studies, which required thousands of GPU hours to train their foundation models in computational pathology [3, 4, 9, 24, 26]. This resource intensive entry-barrier limits open-source advancements in non-resource abundant environments. Thus, we explore feasible solutions to train foundation models at scale on consumer-grade hardware. Our main contributions are as follows:

- To the best of our knowledge, we provide the first comprehensive ablation study that analyzes SSL complexity reductions in relation to weakly supervised classification performance on breast cancer related histopathology tasks.
- We improve over existing semantically relevant contrastive learning methods in computational pathology.
- We show that modifications in data volume, the SSL model architecture and the contrastive learning loss function improve the efficiency of SSL in computational pathology while surpassing state-of-the-art (SOTA) results. The findings of these adaptations enable the utilization of SSL in computational pathology in non-resource abundant environments.

## 2 Methods

We utilized momentum contrast (MoCo)-v3 as our base contrastive SSL framework. Following [26], we chose the tiny Swin Transformer [14] with a convolutional base as the default encoder architecture. In the following we will elucidate the approach and experimental settings for the SSL encoder training and for the evaluation. An overview of the performed experiments can be found in Figure 1.

### 2.1 Contrastive Self-Supervised Learning

For Histopathology tasks, contrastive methods exhibit a decent compromise between performance, simplicity and efficiency [11, 22]. Therefore, we employ the third version of MoCo [6] as the basis for our SSL experiments (Figure 1-A). Following He et al. [10] we interpret contrastive learning as training an encoder for a *dictionary look-up task*:

Let a set of encoded samples  $\{k_0, k_1, k_2, \dots, k_N\}$  be the keys of a dictionary, such that exactly one matching key  $k^+$  exists for a query  $q$ . Then, the contrastive loss is low if  $q$  is similar to  $k^+$  and dissimilar to all other keys. The InfoNCE [18] loss

function is then defined as:

$$\mathcal{L}_{\mathbf{q}} = -\log \frac{\psi(\mathbf{q}, \mathbf{k}^+)}{\psi(\mathbf{q}, \mathbf{k}^+) + \sum_{i=1}^K \psi(\mathbf{q}, \mathbf{k}_i)}, \quad (1)$$

where  $q$  and the corresponding  $k^+$  are the feature vectors belonging to different random augmentations of the same input image and  $K$  is the number of negative samples which is equal to  $N - 1$ , with  $N$  being the batch size or length of the memory queue. The function  $\psi$  is defined as follows:

$$\psi(\mathbf{x}_1, \mathbf{x}_2) = \exp(\text{sim}(\mathbf{x}_1, \mathbf{x}_2)/\tau), \quad (2)$$

where  $\tau$  denotes the temperature parameter and the cosine similarity function is denoted as  $\text{sim}(\cdot)$ . To avoid feature collapse, the keys and queries need to be generated by distinct encoders. Let  $\theta_q$  denote the parameters of the query encoder with the dense projection head, then the parameters of the key encoder  $\theta_k$  are updated as follows:

$$\theta_k \leftarrow m\theta_k + (1 - m)\theta_q, \quad (3)$$

where  $m \in [0, 1)$  is the momentum coefficient. With the key encoder as the exponential average of the query encoder, the key representations stay more consistent which enables a more stabilized training process. We adapted the public MoCo-v3 repository<sup>4</sup> for our experiments to train the tiny Swin Transformer encoders from scratch over 50 epochs using the AdamW [15] optimizer, a learning rate of  $1.5 \cdot 10^{-4}$ , a batch size of 1024 and 40 warm-up epochs. Besides the batch size and the total number of epochs, all other settings remain the default options stated in the documentation of the github repository.

## 2.2 Semantically Relevant Sampling

Wang et al. [26] proposed a self-supervised contrastive learning framework for histopathology called *semantically-relevant contrastive learning (SRCL)*. The main difference between MoCo and SRCL is the increased number of positive samples [6, 26]. Increasing the number of positive samples is of special interest for histopathology tasks as tessellated patches of the same whole slide image (WSI) can exhibit high similarity and should therefore not necessarily be regarded as negative samples during contrastive learning.

**Positive Sampling.** Positive sampling is based on the similarity of the encoded patches and independent on their spatial location in the WSI. Specifically, we sample  $S = 5$  additional positives based on the highest cosine similarity between the key encoder output of an original sample and the other key encoder representations of the augmented samples belonging to a batch or memory queue (cf. Equation 1):

$$\mathcal{L}_{\mathbf{q}} = -\log \frac{\sum_{j=1}^{S+1} \psi(\mathbf{q}, \mathbf{k}_j^+)}{\sum_{j=1}^{S+1} \psi(\mathbf{q}, \mathbf{k}_j^+) + \sum_{i=1}^K \psi(\mathbf{q}, \mathbf{k}_i)}, \quad (4)$$

<sup>4</sup> <https://github.com/facebookresearch/moco-v3>

where  $K = N - S - 1$  and  $\psi$  defined in Equation 2. Following [26] we start the sampling of additional positives after 5 epochs of traditional contrastive learning as the representations need to be meaningful enough such that similar representations relate to similar input patches. We will refer to positive sampling as SRCL following [26].

**Negative Sampling.** Due to the success of positive sampling proposed by Wang et al. [26], we decided to further explore the effects of semantically relevant sampling on the performance of histopathology encoders. We retrieve the  $T = 50$  most dissimilar representations in a batch for each sample. However, instead of ranking the similarity of representations of original patches with representations of augmented patches from the same batch, we rank the similarity of the representations of original patches processed by the key encoder. It is important to observe that this even reduces the computational requirements as you only have to sample one set of logits while in SRCL you have to do it separately for the two different augmented views. The loss function for negative sampling (N-Sam) is updated as follows:

$$\mathcal{L}_{\mathbf{q}} = -\log \frac{\psi(\mathbf{q}, \mathbf{k}^+)}{\psi(\mathbf{q}, \mathbf{k}^+) + \sum_{j=1}^T \psi(\mathbf{q}, \mathbf{k}_j^-) + \sum_{i=1}^K \psi(\mathbf{q}, \mathbf{k}_i)}, \quad (5)$$

with  $K = N - 1$  and  $\psi$  defined in Equation 2.

**Dynamic Sampling.** Because contrasting most similar input patches is unnecessary and distinguishing highly dissimilar samples is trivial, we hypothesize that increasing the weights for the samples of intermediate similarity would be beneficial. Therefore, we propose dynamic sampling (DS), where we increase the number of negative samples by 20 every epoch  $> 5$  and decrease the number of positive sample from 30 to 1 in increments of 5 every epoch  $> 5$ . Furthermore, instead of sampling negative samples from the bottom of the similarity ranking, we sample from the middle of the ranking growing towards both sides. The loss function for DS is as follows:

$$\mathcal{L}_{\mathbf{q}} = -\log \frac{\sum_{j=1}^{S_e+1} \psi(\mathbf{q}, \mathbf{k}_j^+)}{\sum_{j=1}^{S_e+1} \psi(\mathbf{q}, \mathbf{k}_j^+) + \sum_{j=1}^{T_e} \psi(\mathbf{q}, \mathbf{k}_j^-) + \sum_{i=1}^K \psi(\mathbf{q}, \mathbf{k}_i)}, \quad (6)$$

where  $K = N - S - 1$  and  $\psi$  defined in Equation 2, the  $e$  in  $S_e$  and  $T_e$  indicates their dependency on the epoch.

### 2.3 Swin Transformer Modifications

We removed Swin Transformer [14] stages after SSL to extract features from earlier stages and evaluate their informational content on downstream classification tasks. Since the tensor shapes of earlier stages differ from the output dimension we applied 2D adaptive average pooling to retrieve 768 features per patch. Additionally, we concatenated features from all four stages as well as from the last two stages to analyze their combined value for downstream classification tasks.

## 2.4 Evaluation

We follow the STAMP protocol [17] for our data processing pipeline to evaluate the SSL encoders. It consists of two major steps: WSI preprocessing and weakly-supervised training. We resize the images to 0.5 microns per pixel (mpp), use canny edge detection [19] to reject the background and tessellate the tissue part into  $n$  patches of size  $224 \times 224$  pixels. These patches are then processed by an encoder to compress their information to feature vectors of dimension 768. Those embeddings are the result of the WSI-pre-processing and are saved as intermediate files. Next, the weakly supervised training uses those embeddings as inputs to predict a WSI-level categorical target. A ViT model [8] with two layers and 8 attention heads each is used for the supervised multiple-instance learning (MIL) training following Wagner et al. [25]. Since we focus on breast cancer tissue samples, we chose targets with clinical relevance as they are important for prognostic implications. Among the most commonly altered genes with prognostic importance in breast cancer are *TP53*, *CDH1* and *PIK3CA* [1, 13, 20]. Therefore, we evaluate the SSL encoders on the mutation information of those genes. To increase the diversity of our targets even further, we also evaluate our models on metastasis detection in lymph nodes [2]. We use The Cancer Genome Atlas (TCGA)-breast cancer (BRCA) as the training cohort for the genes *TP53*, *CDH1* and *PIK3CA*. The publicly available CAMELYON16 challenge [2] provides internal and external cohorts with the necessary target information about metastasis detection. We use the breast cancer subset of the Clinical Proteomic Tumor Analysis Consortium (CPTAC) as external cohorts for the targets *TP53*, *CDH1* and *PIK3CA*. The ViT MIL models are trained in a weakly-supervised manner on the internal cohort with five-fold cross-validation. Subsequently, the models are deployed on the external cohorts. We report area under the precision recall characteristic (AUPRC) (Table 1) and area under the receiver operating characteristic (AUROC) scores (Table 3) as evaluation metrics, with AUPRC being the main metric due to the data imbalance [25].

## 3 Experimental Results and Discussion

**Data.** We use public datasets throughout this study. For the SSL training, we utilize the breast cancer (BRCA) subset of TCGA ([www.cbioportal.org](http://www.cbioportal.org)) consisting of 1125 hematoxylin and eosin (H&E) stained WSIs. The WSIs are tessellated into patches with 0.5 mpp of size  $512 \times 512$  pixels. After rejecting the background, we retrieve over 4M patches for the SSL training. For the downstream evaluation tasks we employ TCGA-BRCA, the BRCA subset of CPTAC (<https://proteomics.cancer.gov/programs/cptac>) and tissue slides from the CAMELYON16 challenge [2]. An overview of the utilized datasets can be found in Table 2. The performed experiments are visualized in Figure 1-B.

**Our MoCo encoder improves over SOTA results on breast cancer gene classification tasks.** We trained a tiny Swin transformer with MoCo-v3 over

MODEL	CPTAC-BRCA <i>CDH1</i>	CPTAC-BRCA <i>TP53</i>	CPTAC-BRCA <i>PIK3CA</i>	CAMELYON16 TUMOR	AVG
<b>CTransPath</b>	<b>0.991</b>	0.793	0.760	0.683	0.807
MoCo-v3	0.984	0.823	0.790	0.415	0.753
50% data	0.987	0.807	0.795	0.422	0.753
25% data	0.981	0.739	0.764	0.627	0.778
10% data	0.983	0.706	0.751	0.557	0.749
Stage 3	0.973	0.808	0.760	0.759	0.825
Stage 2	0.961	0.686	0.772	0.476	0.724
Stage 1	0.958	0.695	0.726	0.455	0.709
All Stages	0.968	0.798	0.762	0.794	0.830
Last 2	0.972	<b>0.831</b>	0.745	<b>0.811</b>	<b>0.840</b>
SRCL	0.986	0.802	0.778	0.416	0.746
N-Sam	0.983	0.821	<b>0.795</b>	0.436	0.759
DS	0.989	0.783	0.791	0.457	0.755

**Table 1.** Comparison of the encoders deployed on downstream classification tasks. The table contains the average Area Under the Precision Recall Characteristic (AUPRC) over all five Vision Transformer models from the cross validation. SRCL: semantically relevant contrastive learning, N-Sam: negative sampling, DS: dynamic sampling.

half the number of epochs and on only 4% of the WSIs compared to the SOTA CTransPath (CTP) model, and it reaches similar performance on the downstream gene classification tasks (Table 1). On the gene classification targets *TP53* and *PIK3CA*, our model exhibits a superior performance compared to CTP (AUPRC<sub>*TP53*</sub> = 79.3%; AUPRC<sub>*PIK3CA*</sub> = 76.0%) as the results improve +3% in AUPRC for both targets. However, it exhibits substantially worse performance on the metastasis detection task from the CAMELYON16 test set. This drop in performance is presumed to be due to the amplified number of tissue types CTP has been trained on as TCGA even includes lymph node WSIs from axial regions. This is exactly the tissue type utilized for the CAMELYON16 challenge.

**A 50% reduction in SSL training data does not affect downstream gene mutation prediction performance.** With the data reduction experiment we aim to investigate how limiting SSL samples impacts the downstream classification performance (DCP) of them. The potential for the reduction of computational costs is substantial while differences in performance might be negligible [4]. The results show that 50% of the SSL data is adequate to achieve equivalent downstream performance as the 100% baseline (75.3% average AUPRC). Therefore, we can achieve a 50% reduction of computational resources and time without any loss in classification capabilities.

**Incorporating feature representations from previous blocks improves weakly supervised learning performance.** The representations extracted

from the first two stages display inferior performance across all targets. However, our findings demonstrate strongly improved performance on the metastasis detection task for all the models that use the features extracted from the third stage of the encoder (AUPRCs: CTP: 68.3%, MoCo: 41.5%, S3: 75.9%, AS: 79.4%, L2: 81.1%). Although, these encoders exhibit slightly reduced AUPRC scores on *CDH1* compared to CTP and our MoCo baseline, they improve over CTP on *TP53*. Consequently, depending on the task at hand, removing the last stage of the encoder for the feature extraction not only reduces computational costs but also improves classification performance.

**Negative sampling and dynamic sampling improve over semantically relevant contrastive learning.** Our proposed methods DS and N-Sam exhibit the best performance on *PIK3CA* (AUPRC=79.1%, 97.5%) and improve over the MoCo baseline (+2.1%,+4.2% AUPRC) and SRCL (+2%,+4.1% AUPRC) on the metastasis detection task. However, contrary to previous results [26], SRCL does not improve over the MoCo-v3 baseline for our tasks. This could be due to the difference in the tasks at hand. While we evaluate the SSL algorithms utility with weakly supervised MIL tasks, Wang et al. evaluated the benefit of SRCL on a tile based supervised task [26].

## 4 Conclusion

In this work, we analyzed potential avenues to reduce the required resources to train breast cancer WSI encoders in a contrastive self-supervised manner while improving the classification performance on gene mutation and metastasis detection tasks. Our experimental framework enables the benchmarking of a variety of modifications regarding the contrastive SSL based on MoCo-v3 in computational pathology. We examined the influence of data volume adaptations, architecture changes and algorithmic adjustments to analyze their effect on downstream classification tasks while reducing computational complexity. Our findings show that DCP was not effected despite a 50% reduction of SSL data. Furthermore, we demonstrate that removing the last stage of the encoder can enhance performance of weakly supervised learning tasks. Therefore, by reducing the number of parameters, we improve current approaches for feature extraction while making them less computationally expensive. In summary, we provide the methodological insights to enable foundation model training on routinely available data for medical centers across the globe.

## Bibliography

- [1] André, F., Ciruelos, E., Juric, D., et al.: Alpelisib plus fulvestrant for pik3ca-mutated, hormone receptor-positive, human epidermal growth factor receptor-2-negative advanced breast cancer: Final overall survival results from solar-1. *Annals of Oncology* **32**(2), 208–217 (2021)
- [2] Bejnordi, B.E., Veta, M., Van Diest, P.J., et al.: Diagnostic assessment of deep learning algorithms for detection of lymph node metastases in women with breast cancer. *Jama* **318**(22), 2199–2210 (2017)
- [3] Campanella, G., Kwan, R., Fluder, E., et al.: Computational pathology at health system scale – self-supervised foundation models from three billion images (2023)
- [4] Chen, R.J., Ding, T., Lu, M.Y., et al.: A general-purpose self-supervised model for computational pathology (2023)
- [5] Chen, R.J., Krishnan, R.G.: Self-supervised vision transformers learn visual concepts in histopathology (2022)
- [6] Chen, X., Xie, S., He, K.: An empirical study of training self-supervised vision transformers (4 2021), <http://arxiv.org/abs/2104.02057>
- [7] Ding, R., Yadav, A., Rodriguez, E., da Silva, A.C.A.L., Hsu, W.: Tailoring pretext tasks to improve self-supervised learning in histopathologic subtype classification of lung adenocarcinomas. *Computers in Biology and Medicine* **166**, 107484 (2023)
- [8] Dosovitskiy, A., Beyer, L., Kolesnikov, A., Weissenborn, D., Zhai, X., Unterthiner, T., Dehghani, M., Minderer, M., Heigold, G., Gelly, S., Uszkoreit, J., Houlsby, N.: An image is worth 16x16 words: Transformers for image recognition at scale (2021)
- [9] Filiot, A., Ghermi, R., Olivier, A., Jacob, P., Fidon, L., Kain, A.M., Saillard, C., Schiratti, J.B.: Scaling self-supervised learning for histopathology with masked image modeling. *medRxiv* (2023). <https://doi.org/10.1101/2023.07.21.23292757>, <https://www.medrxiv.org/content/early/2023/07/26/2023.07.21.23292757>
- [10] He, K., Fan, H., Wu, Y., Xie, S., Girshick, R.: Momentum contrast for unsupervised visual representation learning (11 2019), <http://arxiv.org/abs/1911.05722>
- [11] Kang, M., Song, H., Park, S., Yoo, D., Pereira, S.: Benchmarking self-supervised learning on diverse pathology datasets (12 2022), <http://arxiv.org/abs/2212.04690>
- [12] Krishnan, R., Rajpurkar, P., Topol, E.J.: Self-supervised learning in medicine and healthcare. *Nature Biomedical Engineering* **6**(12), 1346–1352 (2022)
- [13] Li, S.Y., Rong, M., Grieu, F., Iacopetta, B.: Pik3ca mutations in breast cancer are associated with poor outcome. *Breast cancer research and treatment* **96**, 91–95 (2006)

- [14] Liu, Z., Lin, Y., Cao, Y., Hu, H., Wei, Y., Zhang, Z., Lin, S., Guo, B.: Swin transformer: Hierarchical vision transformer using shifted windows (2021)
- [15] Loshchilov, I., Hutter, F.: Decoupled weight decay regularization (2019)
- [16] Nahhas, O.S.M.E., Loeffler, C.M.L., Carrero, Z.I., et al.: Regression-based deep-learning predicts molecular biomarkers from pathology slides (2023)
- [17] Nahhas, O.S.M.E., van Treeck, M., Wölflein, G., et al.: From whole-slide image to biomarker prediction: A protocol for end-to-end deep learning in computational pathology (2023)
- [18] van den Oord, A., Li, Y., Vinyals, O.: Representation learning with contrastive predictive coding (2019)
- [19] Rong, W., Li, Z., Zhang, W., Sun, L.: An improved canny edge detection algorithm. In: 2014 IEEE international conference on mechatronics and automation. pp. 577–582. IEEE (2014)
- [20] Shiovitz, S., Korde, L.A.: Genetics of breast cancer: a topic in evolution. *Annals of Oncology* **26**(7), 1291–1299 (2015)
- [21] Spasic, I., Nenadic, G., et al.: Clinical text data in machine learning: systematic review. *JMIR medical informatics* **8**(3), e17984 (2020)
- [22] Stacke, K., Unger, J., Lundström, C., Eilertsen, G.: Learning representations with contrastive self-supervised learning for histopathology applications (2022)
- [23] Unger, M., Kather, J.N.: A systematic analysis of deep learning in genomics and histopathology for precision oncology. *BMC Medical Genomics* **17**(1), 48 (2024)
- [24] Vorontsov, E., Bozkurt, A., Casson, A., et al.: Virchow: A million-slide digital pathology foundation model (2023)
- [25] Wagner, S.J., Reisenbüchler, D., West, N.P., et al.: Transformer-based biomarker prediction from colorectal cancer histology: A large-scale multicentric study. *Cancer Cell* (2023)
- [26] Wang, X., Yang, S., Zhang, J., et al.: Transformer-based unsupervised contrastive learning for histopathological image classification. *Medical Image Analysis* **81** (10 2022). <https://doi.org/10.1016/j.media.2022.102559>
- [27] Waqas, A., Bui, M.M., Glassy, E.F., et al.: Revolutionizing digital pathology with the power of generative artificial intelligence and foundation models. *Laboratory Investigation* p. 100255 (2023)
- [28] Wójcik, M.A.: Foundation models in healthcare: Opportunities, biases and regulatory prospects in europe. In: *International Conference on Electronic Government and the Information Systems Perspective*. pp. 32–46. Springer (2022)

## A Supplementary Material

Target	Cohort	i. / e.	#WSI	#feats	#t.o.	C1 #	C2 #
<i>CDH1</i>	TCGA-BRCA	internal	1133	1125	1022	WT 900	MUT 122
<i>TP53</i>	TCGA-BRCA	internal	1133	1125	1022	WT 683	MUT 339
<i>PIK3CA</i>	TCGA-BRCA	internal	1133	1125	1022	WT 686	MUT 336
tumor	CAMELYON16	internal	270	265	265	NO 157	TU 108
<i>CDH1</i>	CPTAC-BRCA	external	653	653	120	WT 112	MUT 8
<i>TP53</i>	CPTAC-BRCA	external	653	653	120	WT 71	MUT 49
<i>PIK3CA</i>	CPTAC-BRCA	external	653	653	120	WT 82	MUT 38
tumor	CAMELYON16	external	129	129	129	NO 80	TU 49

**Table 2.** Overview of the targets used to evaluate the capabilities of the trained encoders. Abbreviations: i. / e. - internal (weakly supervised training) or external (deployment), feats - features (slides processed by the encoder), t.o. - target overlap (intersection between processed slides and available target information), C1 & C2 - available classes, WT - wild-type, MUT - mutated, NO - normal, TU - tumor.

MODEL	CPTAC-BRCA <i>CDH1</i>	CPTAC-BRCA <i>TP53</i>	CPTAC-BRCA <i>PIK3CA</i>	CAMELYON16 TUMOR	AVG
<b>CTransPath</b>	<b>0.894</b>	0.720	0.596	0.686	<b>0.724</b>
MoCo-v3	0.842	<b>0.750</b>	0.647	0.519	0.689
50% data	0.861	0.729	0.648	0.500	0.685
25% data	0.826	0.646	0.613	0.623	0.677
10% data	0.799	0.612	0.585	0.556	0.638
Stage 3 (S3)	0.759	0.713	0.601	0.756	0.708
Stage 2 (S2)	0.632	0.552	0.611	0.528	0.581
Stage 1 (S1)	0.579	0.556	0.545	0.531	0.553
AS	0.729	0.716	0.601	0.779	0.706
L2	0.751	0.750	0.590	<b>0.796</b>	0.722
SRCL	0.846	0.720	0.624	0.545	0.684
N-Sam	0.832	0.738	0.647	0.568	0.696
DS	0.871	0.708	<b>0.654</b>	0.554	0.697

**Table 3.** External AUROC Results. Comparison of the encoders deployed on downstream classification tasks. The table contains the average AUROC over all five ViT models from the cross validation.